Original Article

Anatomic characteristics of primary acquired nasolacrimal duct obstruction: a comparative computed tomography study

Wushuang Wang, Lan Gong[#], Yan Wang[#]

Department of Ophthalmology, Eye, Ear, Nose, and Throat Hospital of Fudan University, Shanghai, China

Contributions: (I) Conception and design: Y Wang; (II) Administrative support: Y Wang, L Gong; (III) Provision of study materials or patients: Y Wang, L Gong; (IV) Collection and assembly of data: All authors; (V) Data analysis and interpretation: W Wang; (VI) Manuscript writing: All authors; (VII) Final approval of manuscript: All authors.

[#]These authors contributed equally for the senior authorship.

Correspondence to: Yan Wang; Lan Gong. Department of Ophthalmology, Eye, Ear, Nose, and Throat Hospital of Fudan University, 83 Fenyang Rd, Xuhui District, Shanghai 200031, China. Email: wangyandoc@163.com; 13501798683@139.com.

Background: Studies of local anatomic characteristics of primary acquired nasolacrimal duct obstruction (PANDO) are important for understanding the etiology of PANDO and guiding surgical treatment. The purpose of this study was to review computed tomography (CT) scans to identify the anatomic differences in the obstructed and unobstructed sides of PANDO patients as well as in control patients in a Chinese population.

Methods: In this retrospective comparative observational study, the CT scans of 126 PANDO patients were reviewed. A total of 76 patients who underwent CT examinations for eyeball atrophy or an intraocular foreign body but had a healthy lacrimal drainage system and orbit structure were enrolled as controls. The nasolacrimal canal (NLC) widths, lacrimal sac fossa structures, and nasal abnormalities in the obstructed and unobstructed sides in patients and both sides in controls were evaluated.

Results: Both obstructed and unobstructed sides in PANDO patients showed significant differences to the sides of controls in NLC width (obstructed: 3.91±0.90 mm, unobstructed: 3.86±0.83 mm, control: 4.31±0.95 mm; obstructed and control: P<0.01, unobstructed and control: P<0.01, respectively), ethmoid sinusitis (26%, 28%, 16%; P=0.03 and P=0.03, respectively), osteomeatal complex opacification (18%, 14%, 7%; P<0.01 and P=0.04, respectively), and agger nasi cell opacification (22%, 20%, 9%; P<0.01 and P<0.01, respectively). However, although no significant differences (all P>0.05) were found between the obstructed and unobstructed sides of unilateral PANDO patients in these characteristics, there were correlations (r=0.714, 0.209, 0.376, and 0.112; P<0.01, P=0.03, P<0.01, P=0.24, respectively). We also found expanded lacrimal sac fossa width (6.45±1.01 mm) and decreased frontal process proportion (45.9%±15.4%) only in the obstructed sides of PANDO patients compared to the lacrimal sac fossa width in controls (6.08±1.16 mm, P<0.01) and the frontal process proportion in controls (49.9%±15.4%, P=0.03). There was no difference in the positional relationship of the uncinate process (UP) with the lacrimal fossa between patients and controls.

Conclusions: A narrow NLC and nasal inflammation are associated with PANDO, while an expanded lacrimal sac fossa and a decreased frontal process proportion could be pathological changes. The healthy sides of unilateral PANDO patients might have a high risk of developing an obstruction. We also found an increased probability of the UP overlapping the lower lacrimal sac fossa in an Asian population compared to the published European data.

Keywords: Nasolacrimal duct obstruction; lacrimal sac fossa; dacryocystorhinostomy (DCR); computed tomography (CT); nasolacrimal canal (NLC)

Submitted Feb 20, 2022. Accepted for publication Aug 07, 2022.
doi: 10.21037/qims-22-170
View this article at: https://dx.doi.org/10.21037/qims-22-170

Introduction

Primary acquired nasolacrimal duct obstruction (PANDO) is a blockage of the lacrimal outflow system that is very clinically common (1). The presence of PANDO can lead to epiphora, mucopurulent discharge, dacryocystitis, and even chronic conjunctivitis (2). The exact causes of PANDO are unknown; however, it is believed to be related to chronic inflammation, fibrosis, and stenosis of the nasolacrimal duct. Computed tomography (CT) is widely used to explore the potential etiology of PANDO and provide guidance for dacryocystorhinostomy (DCR). Previous CT studies have mainly focused on anatomic characteristics of the lacrimal sac fossa, the nasolacrimal canal (NLC), and nasal abnormalities, most of which are still controversial.

The width of the NLC can be easily measured via CT. Some researchers believe that PANDO is related to narrow NLC because the incidence of PANDO is higher in females, who have narrower NLCs than males (3-5). Janssen *et al.* (6) measured the minimum diameter of NLC in 19 PANDO patients and 100 controls and found that PANDO patients had narrower NLCs (3.0 mm) than healthy women (3.35 mm) and men (3.70 mm). However, other studies have drawn opposite conclusions and reported no relationship between NLC width and PANDO through a comparable design (7) or cross-sectional studies in different races (8,9).

The lacrimal sac fossa is formed by the frontal process of the maxillary bone and the lacrimal bone, on which osteotomy is performed during endonasal DCR. The lacrimal sac fossa is bordered by the anterior lacrimal crest of the maxillary bone and the posterior lacrimal crest of the lacrimal bone. The lacrimomaxillary suture is a syndesmotic suture between the frontal process and the lacrimal bone, and is an important landmark for DCR (10). By describing the surgical anatomy and variations, CT can provide important information about the lacrimal sac fossa. For example, lacrimal and maxillary bone thickness have been found to determine the difficulty of osteotomy, and Asian populations have been held to have thicker frontal processes of the maxillary bone than European populations (11). Another important structure is the uncinate process (UP), a thin osseous structure of the lateral nasal cavity. In most cases, the anterior part of UP inserts into the lacrimal bone or the frontal process of the maxillary bone, which means a uncinectomy may be necessary for a successful endonasal DCR osteotomy. A few studies have focused on analyzing the UP position, providing important references for the surgery (11,12). The problem is that some of these CT studies have focused on PANDO patients (12), while others have been based on healthy cases (11,13,14). A comparative design can help reveal any potential change of lacrimal sac fossa structure in PANDO patients, since the disease state itself may lead to bone absorption and remodeling.

A classical CT study about nasal structures and abnormalities in PANDO patients demonstrated a relationship between PANDO and the presence of nasal septal deviation, ethmoidal opacification, and agger nasi cell opacification (15). Opacification could be seen as a radiological feature of inflammation, which has been thought to be etiologically related to PANDO. Using similar methods, other nasal abnormalities have been found to be related to PANDO in different studies, including concha bullosa, inferior concha hypertrophy, osteomeatal complex disease, and maxillary sinusitis (16-19).

In this study, we comprehensively investigated NLC width, lacrimal sac fossa structures, and nasal abnormalities by comparing the obstructed and unobstructed sides of PANDO patients as well as controls. This study provided anatomic information about PANDO in a Chinese population and revealed potential racial variations of nasolacrimal and lacrimal sac fossa structures, giving ophthalmologists more insights into PANDO and DCR surgeries. We presented the following article in accordance with the STROBE reporting checklist (available at https://qims.amegroups.com/article/view/10.21037/qims-22-170/rc).

Methods

Design and patients

In this comparative observational study, we retrospectively reviewed the medical records of PANDO patients and controls who underwent CT examinations in the Eye, Ear, Nose, and Throat (ENT) Hospital of Fudan University between 1 January 2020 and 30 November 2021. The study was conducted in accordance with the Declaration of Helsinki (as revised in 2013). The study was approved by the Ethics Committee of the Eye and ENT Hospital

of Fudan University, and individual consent for this retrospective analysis was waived.

We included PANDO patients over 18 years old who underwent CT scans before DCR, with the diagnosis of PANDO made according to the epiphora symptoms, irrigation tests, diagnostic probing, and CT-dacryocystography (CT-DCG). The obstructed side was defined as complete nasolacrimal duct obstruction confirmed by irrigation tests and CT-DCG. When regurgitation of mucoid or mucopurulent material was found during the irrigation, chronic dacryocystitis was also diagnosed. For the control group, we enrolled patients who underwent CT examinations before surgeries for eyeball atrophy or an intraocular foreign body through frequency matching based on age and gender. For the PANDO group, patients were excluded if they had canalicular obstruction, a history of nasal or lacrimal apparatus surgery, facial fracture and significant trauma, thyroid-associated ophthalmopathy, sinonasal disease, or a tumor. For the control group, besides the exclusion criteria of the PANDO group, we also excluded patients who had partial or complete nasolacrimal duct obstruction (tested by routine preoperative lacrimal irrigation).

CT acquisition and analysis

All CT images of the patients were taken with a multidetector-row CT (Siemens Medical Systems, Erlangen, Germany) in the Eye and ENT Hospital of Fudan University. Transverse scans throughout the orbits and nasal structures were acquired in the helical mode with a tube voltage of 120 kV and a current of 230 mA. The transverse scans were 0.75 mm thick and were converted to 3 mm thick CT sections of coronal planes. Then, we performed the lacrimal irrigation and injected the contrast agent ioversol into the nasolacrimal duct to obtain a CT-DCG. The CT-DCG was only performed in the PANDO group. The images were analyzed with a digital image workstation (Carestream CGRIS; Carestream Health, Rochester, NY, USA). All the CT measurements were performed by one of the authors (WW), who underwent radiological training for lacrimal and nasal CT structures. The methods of measurement used are outlined in subsequent sections of this article.

NLC width

Measurements of NLC width were performed in the bone window (window center, 800 HU; window width, 2,000 HU), including the sectional area of the superior opening of the NLC ($S_{superior}$) and the narrowest NLC width ($D_{minimum}$). Since the nasolacrimal duct is located inferolaterally and slightly posteriorly through the bony NLC to the inferior nasal meatus (10), the axial section of the NLC was an oval shape on the CT scan. We chose the narrowest transverse NLC width as $D_{minimum}$ and measured it on the axial section, which commonly appeared in the middle part of the NLC (*Figure 1A*). We also measured the area of the uppermost NLC opening as $S_{superior}$ on the axial section (*Figure 1B*).

Lacrimal sac fossa structures

The analysis of the lacrimal sac fossa structure was performed through different axial reference levels as reported in previous studies (11,12). In this study, we used two reference levels: the lower level was defined as the lowest axial slice before the lacrimal sac fossa became the NLC, and the middle level was the lowest axial slice in which the middle turbinate inserted into the lateral nasal wall. The upper level was not included since it could not be defined in control scans where a contrast agent was not used. We measured several anatomic paraments of the lacrimal sac fossa according to the relative positions of the anterior extent of the lacrimal sac fossa, the lacrimomaxillary suture, and the posterior lacrimal crest [lines 1, 2, and 3 in *Figure 1C*,*1D*, respectively, show 3 lines perpendicular to the long axis of the lacrimal sac fossa, as per the method described previously (11)]. The lacrimal sac fossa width was the distance from the anterior extent of the lacrimal sac fossa to the posterior lacrimal crest (the distance from lines 1 to 3 in *Figure 1C*). The frontal process proportion in the lacrimal sac fossa was determined as a percentage of the frontal process (the distance from lines 1 to 2) in the lacrimal sac fossa width (the distance from lines 1 to 3; *Figure 1C*). The frontal process thickness was measured at the mid-point between the anterior extent of the lacrimal sac fossa and the lacrimomaxillary suture (*Figure 1D*). The lacrimal bone angle was the angle between the lacrimal bone and the sagittal plane (*Figure 1E*). These anatomic paraments were all measured at the lower level.

We analyzed the UP position at the middle and lower levels. According to the methods reported previously (11,12), the relationship between UP and the lacrimal sac fossa could be categorized into 4 types: position 1, the UP is inserted into the lacrimal bone posterior to the posterior

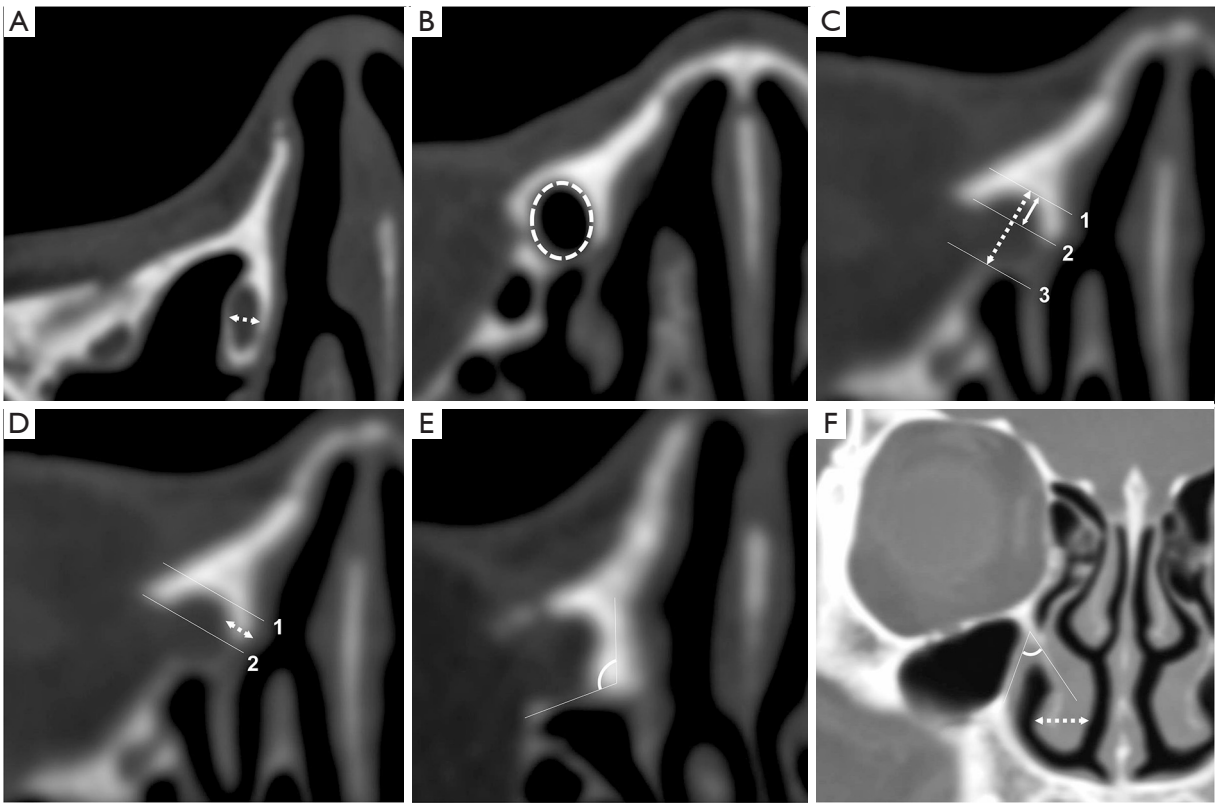

Figure 1 Methods of measurement on the CT scans. (A) The narrowest transverse nasolacrimal canal width ($D_{minimum}$). (B) The sectional area of the uppermost opening of the nasolacrimal canal ($S_{superior}$). (C) The lacrimal sac fossa width (distance from line 1 to 3) and the proportion of the frontal process determined as the percentage of the frontal process (distance from line 1 to 2) in the lacrimal sac fossa width (distance from line 1 to 3). (D) The thickness of the frontal process of the maxillary bone was measured at the mid-point between line 1 and line 2. (E) The angle between the lacrimal bone and the sagittal plane. (F) Inferior turbinate thickness and inferior turbinate angle, the angle between bony inferior turbinate and medial wall of the maxillary sinus. Arrow (↔): distance. Circle (○): area. Line 1: anterior extent of the lacrimal sac fossa. Line 2: maxillary-lacrimal line. Line 3: posterior lacrimal crest. CT, computed tomography.

lacrimal crest (retrolacrimal position); position 2, the UP is inserted into the lacrimal bone anterior to the posterior lacrimal crest (lacrimal position); position 3, the UP is inserted into the frontal process of the maxillary bone (maxillary position); and position 4, the UP is inserted into the middle turbinate (turbinal position). Among these positions, the UP in positions 2 and 3 overlaps the lacrimal sac fossa and can influence the endonasal DCR, but this does not occur in positions 1 and 4. Based on this classification, we compared the UP position distributions in our study with the published data to find the potential difference in the presence of overlap.

Nasal structures and abnormalities

This study applied widely used methods to measure the nasal quantitative structure. Two nasal structure parameters were measured on the coronary section according to previously reported methods (20,21), including inferior turbinate thickness and inferior turbinate angle (the angle between the bony inferior turbinate and the medial wall of the maxillary sinus), which reflected the relative position of the inferior turbinate (*Figure 1F*). Nasal abnormalities included nasal septal deviation, concha bullosa, and the inflammation of the frontal sinus, maxillary sinus, ethmoid sinus, osteomeatal complex (the common channel linking the frontal sinus, anterior ethmoid air cells, and the maxillary sinus to the middle meatus), and agger nasi cells (the most anterior ethmoidal air cells lying inferior to the frontal recess). For the purposes of this study, moderate-to-severe nasal septal deviation was included. Nasal inflammation was defined as signs of mucosal thickening or

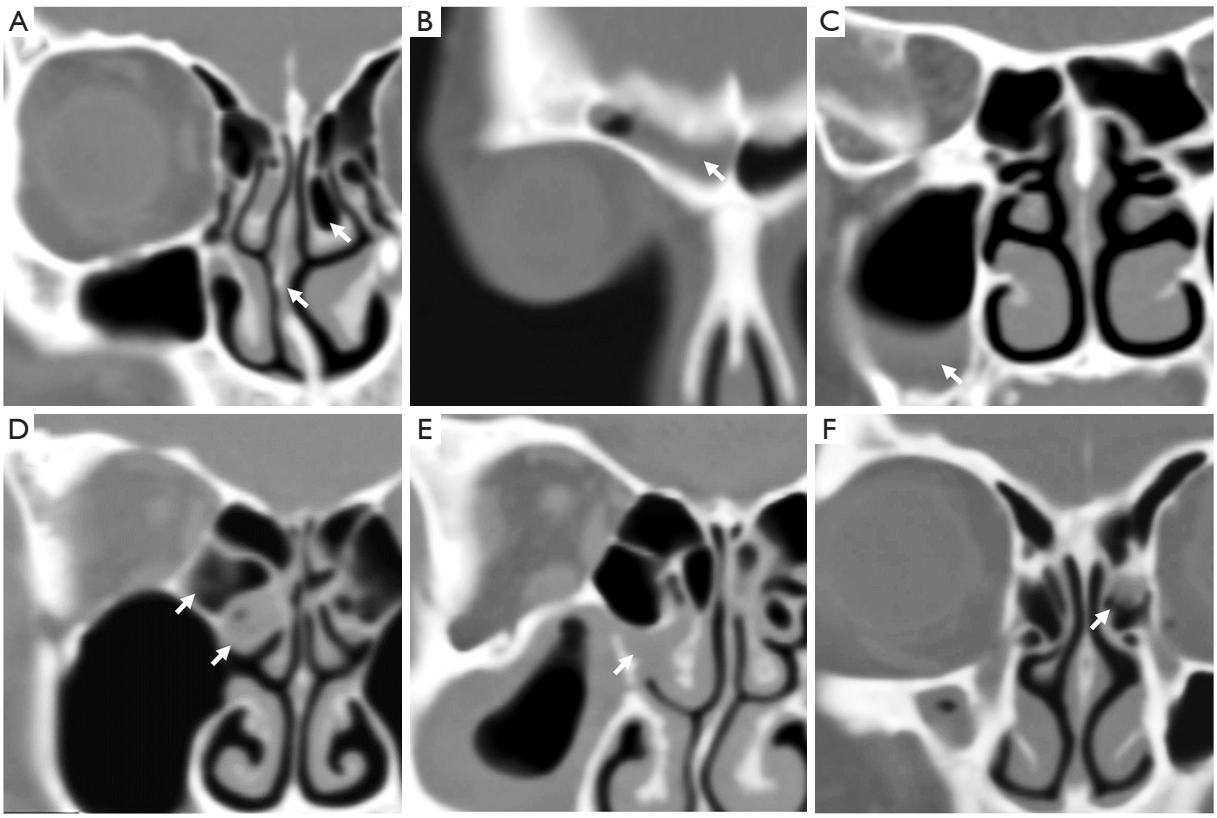

Figure 2 Typical CT images of nasal abnormalities in the coronal plane. (A) Nasal septal deviation and concha bullosa. (B) Frontal sinusitis. (C) Maxillary sinusitis. (D) Ethmoid sinusitis. (E) Osteomeatal complex opacification. (F) Agger nasi cell opacification. Arrows: critical nasal abnormalities. CT, computed tomography.

opacification of the certain sinus or air cell on the CT scan (*Figure 2*).

Statistical analysis

Statistical data were analyzed using SPSS 19.0 (IBM Corp., Chicago, IL, USA). Results were expressed as means ± standard deviation (SD) or percentage. We used the *t*-test (NLC width, lacrimal sac fossa structure, nasal structures), chi-squared test (nasal abnormalities), and Fisher's exact test (UP position) to find differences between PANDO patients and controls. The analysis compared the controls with the obstructed sides of PANDO patients, as well as the controls and the unobstructed sides of the PANDO patients. We used a paired *t*-test and the McNemar test to further determine whether they differed in the obstructed and unobstructed sides of patients with unilateral PANDO. The Pearson correlation coefficient was calculated. Multiple chi-squared tests and Bonferroni post hoc comparisons were used to compare the UP positions in this study with other published data. Differences were considered significant at a level of $P<0.05$.

Results

A total of 126 CT scans of PANDO patients were studied after excluding those with histories of orbit fracture (n=2), nasal surgeries (n=2), and lacrimal apparatus surgeries (n=8) from the 138 available cases. Among them, the data of 107 patients was complicated by chronic dacryocystitis (84.9%). There were 15 PANDO patients with bilateral obstruction, and the other 111 had unilateral obstruction (i.e., 141 obstructed sides and 111 unobstructed sides). The CT scans of 76 patients (55 with eyeball atrophy and 21 with an intraocular foreign body) were enrolled as controls (i.e., 152 control sides) after excluding those with histories of fractures, tumors, surgery, and obstructed nasolacrimal ducts. The distribution of age and gender was balanced: the

Table 1 Demographic data of PANDO patients and the control group

Variables	PANDO (n=126)	Control (n=76)	P value
Age, years (mean ± SD)	54.11±12.21	53.34±11.67	0.66
Gender, n (%)			0.78
Male	26 (20.6)	17 (22.4)	
Female	100 (79.4)	59 (77.6)	
Clinical history	With chronic dacryocystitis, n=107	Eyeball atrophy, n=55	
	Without chronic dacryocystitis, n=19	Intraocular foreign body, n=21	

PANDO, primary acquired nasolacrimal duct obstruction.

mean age was 54.11±12.21 years in the PANDO group and 53.34±11.67 years in the control group (P=0.66). The male-to-female ratio was 1:3.85 in the PANDO group and 1:3.47 in the control group (P=0.78; *Table 1*).

Comparisons of NLC width

We found narrower NLC widths in both the obstructed sides and unobstructed sides in the PANDO group than in those of the control group (*Table 2*). We measured NLC width in two positions, and $D_{minimum}$ showed a significant difference. The mean $D_{minimum}$ was 3.91±0.90 mm in the obstructed side, 3.86±0.83 mm in the unobstructed side, and 4.31±0.95 mm in the control group (all P<0.01). No statistical difference was found in $S_{superior}$ (24.47±7.62 mm^2 in the obstructed side, 23.08±7.58 mm^2 in the unobstructed side, and 23.56±7.70 mm^2 in control; P=0.31 and 0.62, respectively). In unilateral PANDO, mean $D_{minimum}$ was 3.93±0.94 mm in the obstructed side and 3.86±0.83 mm in the unobstructed side, but the difference was not significant (P=0.25). A strong correlation was found between the NLC widths of bilateral sides (r=0.714; P<0.01; *Table 3*).

Comparisons of lacrimal sac fossa structures

A larger lacrimal sac fossa width was found in the obstructed side (6.45±1.01 mm) than in the control side (6.08±1.16 mm) with a significant difference (P<0.01), and lacrimal sac fossa width was 6.23±1.02 mm in the unobstructed side without significance (P=0.28). A similar result was found in the frontal process proportion. The frontal process of the maxillary bone accounted for a lower proportion of lacrimal sac fossa in the obstructed side (45.9%±15.4%) than the control side (49.9%±15.4%; P=0.03) but not in the unobstructed side (47.0%±15.8%) compared with the control side (P=0.13). However, frontal process thickness and lacrimal bone angle showed no difference between the PANDO and control groups (*Table 2*).

Consistent with the previous results, in patients with unilateral PANDO, lacrimal sac fossa width was larger in the obstructed side (6.48±1.01 mm) than on the unobstructed side (6.23±1.02 mm; P<0.01). The frontal process proportion showed no difference in patients with unilateral PANDO (obstructed, 45.9%±15.8%; unobstructed, 47.0%±15.8%; P=0.38). Both showed correlations (lacrimal sac fossa width, r=0.610, P<0.01; frontal process proportion, r=0.705, P<0.01) between bilateral sides (*Table 3*).

The proportions of UP in positions 1, 2, 3, and 4 were 2%, 29%, 41%, and 28%, respectively, in the obstructed side, 2%, 25%, 45%, and 28%, respectively, in the unobstructed side, and 2%, 28%, 51%, and 19%, respectively, in controls at the middle level. At the lower level, the proportions of UP in positions 1, 2, 3, and 4 were 5%, 84%, 11%, and 0, respectively, in the obstructed side, 5%, 83%, 12%, and 0, respectively, in the unobstructed side, and 6%, 82%, 12%, and 0, respectively, in controls (*Figure 3*). There was no difference in UP position distributions between patients and controls in the middle (obstructed and control: P=0.22, unobstructed and control: P=0.40, respectively) and lower lacrimal sac fossa levels (P=0.93 and 1.00, respectively). Subsequently, we analyzed the UP position distributions in all 404 sides of the 202 people (*Table 4*). At the middle level, most UP (n=185, 45.8%) were inserted into the frontal process of the maxillary bone. Others were inserted into the lacrimal bone (n=112, 27.7%) and the middle turbinate (n=99, 24.5%), and only 8 (2.0%) were inserted into the lacrimal bone posterior to the posterior lacrimal crest. At the lower level, less were found located in the frontal process (n=11.4%),

Table 2 Comparisons of the anatomic structures and abnormalities on CT scans between the PANDO and the control groups

Variables	PANDO		Control side (n=152)	P†	
	Obstructed side (n=141)	Unobstructed side (n=111)		O-C	U-C
Nasolacrimal canal width (mean ± SD)					
$S_{superior}$ (mm^2)	24.47±7.62	23.08±7.58	23.56±7.70	0.31	0.62
$D_{minimum}$ (mm)	3.91±0.90	3.86±0.83	4.31±0.95	<0.01*	<0.01*
Lacrimal sac fossa structure (mean ± SD)					
Lacrimal sac fossa width (mm)	6.45±1.01	6.23±1.02	6.08±1.16	<0.01*	0.28
Frontal process proportion (%)	45.9±15.4	47.0±15.8	49.9±15.4	0.03*	0.13
Frontal process thickness (mm)	2.52±0.54	2.42±0.58	2.51±0.58	0.93	0.20
Lacrimal bone angle (°)	120.02±10.91	120.64±9.68	121.20±11.37	0.37	0.67
Nasal structures (mean ± SD)					
Inferior turbinate thickness (mm)	8.78±2.10	8.72±1.98	8.85±2.06	0.77	0.61
Inferior turbinate angle (°)	57.39±16.47	59.89±16.20	62.30±15.97	0.01*	0.26
Nasal abnormalities					
Nasal septal deviation	31 (22%)	26 (23%)	33 (22%)	0.95	0.74
Concha bullosa	42 (30%)	32 (29%)	33 (22%)	0.11	0.19
Frontal sinusitis	2 (1%)	4 (4%)	4 (3%)	0.75	0.93
Maxillary sinusitis	32 (23%)	25 (23%)	32 (21%)	0.73	0.78
Ethmoid sinusitis	37 (26%)	31 (28%)	24 (16%)	0.03*	0.03*
Osteomeatal complex opacification	25 (18%)	16 (14%)	10 (7%)	<0.01*	0.04*
Agger nasi cell opacification	31 (22%)	22 (20%)	13 (9%)	<0.01*	<0.01*

$S_{superior}$, sectional area of the superior opening of the nasolacrimal canal; $D_{minimum}$, narrowest NLC width. †, *t*-test (measurement data) and chi-square test (nasal abnormalities) between the obstructed sides and the control sides as well as the unobstructed sides and the control sides. *, P<0.05. CT, computed tomography; PANDO, primary acquired nasolacrimal duct obstruction; O, obstructed side of PANDO; U, unobstructed side of PANDO; C, control; SD, standard deviation.

Table 3 Comparisons of the critical characteristics within unilateral PANDO

Variables	Obstructed side (n=111)	Unobstructed side (n=111)	P†	r‡	P (r)
Nasolacrimal canal and lacrimal sac fossa structures (mean ± SD)					
$D_{minimum}$ (mm)	3.93±0.94	3.86±0.83	0.25	0.714	<0.01*
Lacrimal sac fossa width (mm)	6.48±1.01	6.23±1.02	<0.01*	0.610	<0.01*
Frontal process proportion (%)	45.9±15.8	47.0±15.8	0.38	0.705	<0.01*
Inferior turbinate angle (°)	58.62±16.88	59.89±16.20	0.31	0.718	<0.01*
Nasal abnormalities					
Ethmoid sinusitis	27 (24%)	31 (28%)	0.61	0.209	0.03*
Osteomeatal complex opacification	18 (16%)	16 (14%)	0.82	0.376	<0.01*
Agger nasi cell opacification	23 (21%)	22 (20%)	1.00	0.112	0.24

†, Paired *t*-test and McNemar test within unilateral PANDO patients; ‡, Pearson correlation coefficient is calculated with P values; *, P<0.05. $D_{minimum}$, narrowest NLC width; PANDO, primary acquired nasolacrimal duct obstruction; SD, standard deviation.

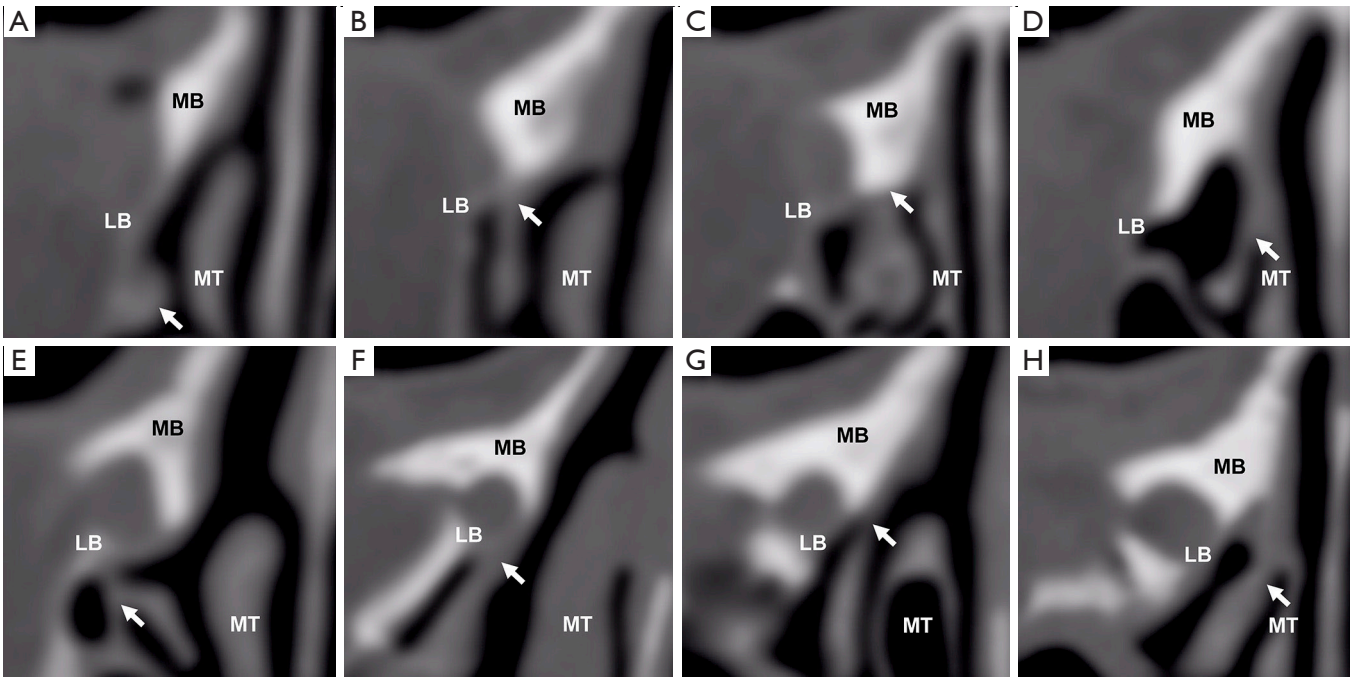

Figure 3 Positions of insertion of the UP into the lacrimal sac fossa. (A-D) Show the UP positions at the middle level (the lowest axial slice in which the middle turbinate is inserted into the lateral nasal wall) and (E-H) were at the lower level (the lowest axial slice before the nasolacrimal canal became lacrimal sac fossa). At the middle level, UP was found to insert into position 1 (A), position 2 (B), position 3 (C), and position 4 (D). Similarly, UP was inserted into position 1 (E), position 2 (F), position 3 (G), and position 4 (H) at the lower level. Arrows: uncinate process. Positions 1, 2, 3, and 4: UP inserted into the lacrimal bone posterior to the posterior lacrimal crest, into the lacrimal bone anterior to the posterior lacrimal crest, into the frontal process of maxillary bone, and into the middle turbinate, respectively. MB, maxillary bone; LB, lacrimal bone; MT, middle turbinate; UP, uncinate process.

Table 4 Comparisons of the position of the unciform process in the current study and the published data (11,12)

Variables	Position† 1: retrolacrimal	Position 2: lacrimal	Position 3: maxillary	Position 4: turbinal
UP position at the middle level, n (%)				
French (12)	4 (5.2)	18 (23.4)	43 (55.8)	12 (15.6)
Korean (11)	0 (0)	17 (11.1)	98 (64.5)	37 (24.3)
Chinese	8 (2.0)	112 (27.7)	185 (45.8)	99 (24.5)
UP position at the lower level, n (%)				
French	25 (32.5)	35 (45.5)	17 (22.0)	0 (0)
Korean	0 (0)	122 (80.3)	30 (19.7)	0 (0)
Chinese	22 (5.4)	335 (82.9)	46 (11.4)	1 (0.3)

†, positions 1, 2, 3, and 4: up inserts into the lacrimal bone posterior to the posterior lacrimal crest, into the lacrimal bone anterior to the posterior lacrimal crest, into the frontal process of maxillary bone, and into the middle turbinate, respectively. UP, unciform process.

and more were located in the lacrimal bone (n=335, 82.9%). In 22 cases (5.4%), UP was found in the retrolacrimal position, and only 1 (0.3%) was in the middle turbinate position.

By comparing our results with the published data (11,12), we found that a French population had a significantly

Table 5 Comparisons of the proportion of the uncinate process overlapping with the lacrimal sac fossa in Asian and European populations (11,12)

Variables	French (12) (n=77)	Korean (11) (n=152)	Chinese (n=404)	P‡
UP position at the middle level, n (%)				0.55
Positions† 1 and 4: not overlapping	16 (20.8)	37 (24.3)	107 (26.5)	
Positions 2 and 3: overlapping	61 (79.2)	115 (75.7)	297 (73.5)	
UP position at the lower level, n (%)				<0.01*
Positions 1 and 4: not overlapping	25 (32.5)[a]	0 (0.0)[b]	23 (5.4)[c]	
Positions 2 and 3: overlapping	52 (67.5)[a]	152 (100.0)[b]	401 (94.6)[c]	

†, positions 1 and 4 indicate that the UP did not overlap the lacrimal sac fossa, while 2 and 3 indicate overlapping; ‡, Chi-square tests in the difference of UP position among different countries. [abc], Bonferroni *post hoc* multiple comparisons: UP positions differ from each other among the three counties at the lower level. *, P<0.05. UP, unciform process.

higher proportion of UP at positions 1 and 4 (32.5%) than populations in Korea (0.0%; Bonferroni adjusted P<0.01) and China (5.4%; Bonferroni adjusted P<0.01) at the lower level. However, no statistical difference was found at the middle level among different races (P=0.55; *Table 5*).

Comparisons of nasal structures and abnormalities

The PANDO group showed more nasal inflammatory changes than in the control group, including ethmoid sinusitis (26% in the obstructed side, 28% in the unobstructed side, and 16% in the control side), osteomeatal complex opacification (18% in the obstructed side, 14% in the unobstructed side, and 7% in the control side), and agger nasi cell opacification (22% in the obstructed side, 20% in the unobstructed side, and 9% in the control side). All these differences were significant. A narrower inferior turbinate angle was found in the PANDO group but only in the obstructed side (57.39°±16.47°; control, 62.30°±15.97°; P=0.01). We did not find more nasal septal deviation, concha bullosa, frontal sinusitis, or maxillary sinusitis in the PANDO group, nor did we find any difference in the inferior turbinate thickness (*Table 2*). As seen with NLC width, in the paired tests within unilateral PANDO patients, the obstructed side and the unobstructed side had a similar nasal abnormality ratio in ethmoid sinusitis (24% in the obstructed side, 28% in the unobstructed side; P=0.61), osteomeatal complex opacification (16% in the obstructed side, 14% in the unobstructed side; P=0.82), and agger nasi cell opacification (21% in the obstructed side, 20% in the unobstructed side; P=1.00). Except for agger nasi cell opacification, we found positive correlations in ethmoid sinusitis (r=0.209; P=0.03) and osteomeatal complex opacification (r=0.376; P<0.01) between the bilateral sides (*Table 3*).

Discussion

This study provided anatomic information related to PANDO in a Chinese population. Our study supported the opinion that PANDO patients tend to have narrower NLCs and more nasal inflammation than the healthy population. Further, there was no difference among unilateral PANDO patients between the obstructed and unobstructed sides. By comparing our findings with other published data, we also found some potential anatomic differences between Chinese patients and other ethnicities, especially in the UP position.

A main finding of this study was that anatomic differences were only found with significance between the PANDO group and the control group, but not between the obstructed and unobstructed sides within patients with unilateral PANDO. These differences included NLC width, inferior turbinate angle, ethmoid sinusitis, osteomeatal complex opacification, and agger nasi cell opacification. For example, NLC width in the unobstructed side appeared equal to the obstructed side and showed a strong correlation. In other words, similar NLC widths, inferior turbinate angle, and nasal inflammatory states were found in the bilateral sides of PANDO patients, no matter whether they were obstructed or not. We suggest this may be because the skeletal developments determine the similarity of bilateral NLC widths, while the nasal inflammatory states may also affect the other side. Many PANDO patients developed bilateral obstruction several years after the initial diagnosis of unilateral obstruction. If we consider narrow NLC width and nasal inflammation as risk factors for

PANDO, we can assume an increased risk of obstruction in the healthy side of a patient with unilateral PANDO due to the strong correlation. Of course, it is difficult for this cross-sectional study to give a rigorous conclusion. Further research is needed to provide more insights into the etiology of PANDO.

The lacrimal sac fossa width expanded only in the obstructed side, and statistical significance was found between the lacrimal sac fossa width in obstructed side and the unobstructed side. A possible explanation for this is that the expanded lacrimal sac could exert a chronic and maintained compression on the bone (bone remodeling), or the inflammation of chronic dacryocystitis leads to bone absorption, which does not exist in the unobstructed side. Similarly, active bone remodeling was observed in the bone fragments after DCR (22). We also found a slightly smaller proportion of frontal process in the obstructed side, probably due to the expansion of the lacrimal sac fossa. The thickness of the frontal process seemed unchanged in the PANDO group. These anatomic changes could be regarded as a consequential pathological change of lacrimal structure in patients with PANDO. The lacrimal bone angle did not differ between the PANDO group and the control group, indicating that the shape of the lacrimal sac fossa is not related to PANDO.

Notably, the sectional area of the superior opening of the NLC ($S_{superior}$) showed no difference between the PANDO and control groups. Instead, it seemed larger in the obstructed side than in the unobstructed and in the control group, although without significance. This may be because the expansion of the lacrimal sac fossa impacted the uppermost opening of NLC, making it a less appropriate NLC width measuring method compared to the minimum diameter. We also found a narrower inferior turbinate angle in the PANDO group, consistent with the previous study (21). While it is still uncertain how the narrower inferior turbinate angle is related to the obstruction, this may be because the narrower inferior turbinate angle affects the opening site of the lacrimal drainage system. In contrast to some previous results (15,17-20), nasal septal deviation, concha bullosa, and inferior turbinate thickness were found to be not associated with PANDO. The prevalence of sinus inflammation shown by CT in the healthy controls was similar to the result of a previous study (23).

Our study was based on a Chinese population, and we also compared the results here with studies of other populations. Studies of lacrimal sac fossa variations could guide endonasal DCR. Positions of UP on the lacrimal sac fossa have been widely discussed, for example, in a Korean study (11) based on healthy controls and a French (12) study based on PANDO patients. In our study, we found no difference in UP position between the PANDO and control group, which indicated that the presence of nasolacrimal duct obstruction had nothing to do with the UP position. Thus, we could compare the UP position in different studies regardless of whether the study was based on participants with or without obstruction. The Korean and French studies and our study were all included in the comparison. To simplify the analysis, we divided the UP position into two groups: group 1 included positions 1 and 4 in which UP did not overlap with the lacrimal sac fossa, and a uncinectomy was less necessary during endonasal DCR, and group 2 included positions 2 and 3 in which UP overlapped with the lacrimal sac fossa and a uncinectomy was more necessary. We found that, at the lower level, the French population had a significantly higher proportion of UP attached to positions 1 and 4 than the Korean and Chinese groups. These results showed an increased probability of UP overlapping the lower lacrimal sac fossa in Asian populations than European populations, indicating that uncinectomy may be more necessary during DCR in Asian populations.

Generally, the Chinese population had a relatively wide NLC. Healthy Chinese males and females had a mean narrowest NLC width of 4.89 and 4.17 mm, respectively, in this study; it was 3.52 and 3.36 mm, respectively, in the Nigerian population (5); 3.70 and 3.35 mm, respectively, in people from the Netherlands (6); 3.9 and 3.6 mm, respectively, in New Zealanders (9); and 4.7 and 4.2 mm, respectively, in Caucasian populations in Turkey (24,25). Regarding the lacrimal sac fossa structure, the mean thickness of the frontal process of maxillary bone at the mid-point in healthy Chinese males and females was 2.71 and 2.45 mm, respectively, in this study. This was thicker than the data reported in a Korean population (2.34 mm in males and 2.02 mm in females) and a Japanese population (2.18 mm in males and 2.17 mm in females), which were measured using the same method as used in our study, indicating a greater challenge in the osteotomy during endonasal DCR in the Chinese population than in other populations (13,14). The mean proportion of the frontal process in this study (50%) was similar to the Korean study (57%) (13).

This study had some limitations. (I) Manual measurement was used in this study, which was time-consuming and presented a risk of bias. (II) The study was

a cross-sectional design, from which it was hard to make a causal inference. (III) The controls recruited to this study were patients diagnosed with eyeball atrophy or an intraocular foreign body because CT scans of "completely healthy" people were hard to acquire in our hospital. (IV) The CT-DCG was only performed in the PANDO group.

In conclusion, we found that PANDO patients had narrower NLC widths and more nasal inflammation compared with healthy controls. An expanded lacrimal sac fossa and a decreased frontal process proportion were the pathological changes of the obstructed sides in PANDO patients. We supposed that the healthy sides of unilateral PANDO patients might have a high risk of obstruction. The Asian population had a higher percentage of UP overlapping the lower lacrimal sac fossa compared to the published European data.

Acknowledgments

Funding: None.

Footnote

Reporting Checklist: The authors have completed the STROBE reporting checklist. Available at https://qims.amegroups.com/article/view/10.21037/qims-22-170/rc

Conflicts of Interest: All authors have completed the ICMJE uniform disclosure form (available at https://qims.amegroups.com/article/view/10.21037/qims-22-170/coif). The authors have no conflicts of interest to declare.

Ethical Statement: The authors are accountable for all aspects of the work in ensuring that questions related to the accuracy or integrity of any part of the work are appropriately investigated and resolved. The study was conducted in accordance with the Declaration of Helsinki (as revised in 2013). The study was approved by the Ethics Committee of the Eye, Ear, Nose, and Throat Hospital of Fudan University, and individual consent for this retrospective analysis was waived.

References

1. Bartley GB. Acquired lacrimal drainage obstruction: an etiologic classification system, case reports, and a review of the literature. Part 1. Ophthalmic Plast Reconstr Surg 1992;8:237-42.
2. Ali MJ, Patnaik S, Kelkar N, Ali MH, Kaur I. Alteration of Tear Cytokine Expressions in Primary Acquired Nasolacrimal Duct Obstruction - Potential Insights into the Etiopathogenesis. Curr Eye Res 2020;45:435-9.
3. Shigeta K, Takegoshi H, Kikuchi S. Sex and age differences in the bony nasolacrimal canal: an anatomical study. Arch Ophthalmol 2007;125:1677-81.
4. Ramey NA, Hoang JK, Richard MJ. Multidetector CT of nasolacrimal canal morphology: normal variation by age, gender, and race. Ophthalmic Plast Reconstr Surg 2013;29:475-80.
5. Groessl SA, Sires BS, Lemke BN. An anatomical basis for primary acquired nasolacrimal duct obstruction. Arch Ophthalmol 1997;115:71-4. Erratum in: Arch Ophthalmol 1997;115:655.
6. Janssen AG, Mansour K, Bos JJ, Castelijns JA. Diameter of the bony lacrimal canal: normal values and values related to nasolacrimal duct obstruction: assessment with CT. AJNR Am J Neuroradiol 2001;22:845-50.
7. Takahashi Y, Nakata K, Miyazaki H, Ichinose A, Kakizaki H. Comparison of bony nasolacrimal canal narrowing with or without primary acquired nasolacrimal duct obstruction in a Japanese population. Ophthalmic Plast Reconstr Surg 2014;30:434-8.
8. Fasina O, Ogbole GI. CT assessment of the nasolacrimal canal in a black African Population. Ophthalmic Plast Reconstr Surg 2013;29:231-3.
9. McCormick A, Sloan B. The diameter of the nasolacrimal canal measured by computed tomography: gender and racial differences. Clin Exp Ophthalmol 2009;37:357-61.
10. Cohen AJ, Mercandetti M, Brazzo B. The Lacrimal System: Diagnosis, Management, and Surgery, Second Edition. 2015.
11. Woo KI, Maeng HS, Kim YD. Characteristics of intranasal structures for endonasal dacryocystorhinostomy in asians. Am J Ophthalmol 2011;152:491-498.e1.
12. Fayet B, Racy E, Assouline M, Zerbib M. Surgical anatomy of the lacrimal fossa a prospective computed

tomodensitometry scan analysis. Ophthalmology 2005;112:1119-28.
13. Kang D, Park J, Na J, Lee H, Baek S. Measurement of Lacrimal Sac Fossa Using Orbital Computed Tomography. J Craniofac Surg 2017;28:125-8.
14. Sarbajna T, Takahashi Y, Valencia MRP, Ito M, Nishimura K, Kakizaki H. Computed tomographic assessment of the lacrimal sac fossa in the Japanese population. Ann Anat 2019;224:23-7.
15. Kallman JE, Foster JA, Wulc AE, Yousem DM, Kennedy DW. Computed tomography in lacrimal outflow obstruction. Ophthalmology 1997;104:676-82.
16. Borges Dinis P, Oliveira Matos T, Ângelo P. Does sinusitis play a pathogenic role in primary acquired obstructive disease of the lachrymal system? Otolaryngol Head Neck Surg 2013;148:685-8.
17. Habesoglu M, Eriman M, Habesoglu TE, Kinis V, Surmeli M, Deveci I, Deveci S. Co-occurrence and possible role of sinonasal anomalies in primary acquired nasolacrimal duct obstruction. J Craniofac Surg 2013;24:497-500.
18. Yazici H, Bulbul E, Yazici A, Kaymakci M, Tiskaoglu N, Yanik B, Ermis S. Primary acquired nasolacrimal duct obstruction: is it really related to paranasal abnormalities? Surg Radiol Anat 2015;37:579-84.
19. Samarei R, Samarei V, Aidenloo NS, Fateh N. Sinonasal Anatomical Variations and Primary Acquired Nasolacrimal Duct Obstruction: A Single Centre, Case-Control Investigation. Eurasian J Med 2020;52:21-4.
20. Dikici O, Ulutaş HG. Relationship Between Primary Acquired Nasolacrimal Duct Obstruction, Paranasal Abnormalities and Nasal Septal Deviation. J Craniofac Surg 2020;31:782-6.
21. Gul A, Aslan K, Karli R, Ariturk N, Can E. A Possible Cause of Nasolacrimal Duct Obstruction: Narrow Angle Between Inferior Turbinate and Upper Part of the Medial Wall of the Maxillary Sinus. Curr Eye Res 2016;41:729-33.
22. Hinton P, Hurwitz JJ, Cruickshank B. Nasolacrimal bone changes in diseases of the lacrimal drainage system. Ophthalmic Surg 1984;15:516-21.
23. Nazri M, Bux SI, Tengku-Kamalden TF, Ng KH, Sun Z. Incidental detection of sinus mucosal abnormalities on CT and MRI imaging of the head. Quant Imaging Med Surg 2013;3:82-8.
24. Ulutas HG, Yazici B, Ulutas E, Yazici Z. Nasolacrimal canal morphology with or without idiopathic obstruction in Caucasian adults: a multidetector CT study. Int Ophthalmol 2022;42:1727-35.
25. Bulbul E, Yazici A, Yanik B, Yazici H, Demirpolat G. Morphometric Evaluation of Bony Nasolacrimal Canal in a Caucasian Population with Primary Acquired Nasolacrimal Duct Obstruction: A Multidetector Computed Tomography Study. Korean J Radiol 2016;17:271-6.

Cite this article as: Wang W, Gong L, Wang Y. Anatomic characteristics of primary acquired nasolacrimal duct obstruction: a comparative computed tomography study. Quant Imaging Med Surg 2022;12(11):5068-5079. doi:10.21037/qims-22-170

